



**HAL**  
open science

## Rate of decrease of the specific surface area of dry snow: Isothermal and temperature gradient conditions

Anne-Sophie Taillandier, Florent Domine, William R. Simpson, Matthew Sturm, Thomas A. Douglas

### ► To cite this version:

Anne-Sophie Taillandier, Florent Domine, William R. Simpson, Matthew Sturm, Thomas A. Douglas. Rate of decrease of the specific surface area of dry snow: Isothermal and temperature gradient conditions. *Journal of Geophysical Research: Earth Surface*, 2007, 112 (F03003), 1 à 13 p. 10.1029/2006JF000514 . insu-00377486

**HAL Id: insu-00377486**

**<https://insu.hal.science/insu-00377486>**

Submitted on 11 Mar 2021

**HAL** is a multi-disciplinary open access archive for the deposit and dissemination of scientific research documents, whether they are published or not. The documents may come from teaching and research institutions in France or abroad, or from public or private research centers.

L'archive ouverte pluridisciplinaire **HAL**, est destinée au dépôt et à la diffusion de documents scientifiques de niveau recherche, publiés ou non, émanant des établissements d'enseignement et de recherche français ou étrangers, des laboratoires publics ou privés.

## Rate of decrease of the specific surface area of dry snow: Isothermal and temperature gradient conditions

Anne-Sophie Taillandier,<sup>1</sup> Florent Domine,<sup>1</sup> William R. Simpson,<sup>2,3</sup> Matthew Sturm,<sup>4</sup>  
and Thomas A. Douglas<sup>4</sup>

Received 31 March 2006; revised 16 January 2007; accepted 15 March 2007; published 14 July 2007.

[1] The specific surface area (SSA) of snow is the surface area available to gases per unit mass. It is an important variable for quantifying air-snow exchange of chemical species, and it is closely related to other variables such as albedo. Snow SSA decreases during metamorphism, but few data are available to quantify its rate of decrease. We have performed laboratory experiments under isothermal and temperature gradient conditions during which the SSA of snow samples was monitored for several months. We have also monitored the SSA of snowfalls subjected to large temperature gradients at a field site in the central Alaskan taiga. The same snow layers were also monitored in a manipulated snowpack where the temperature gradient was greatly reduced. In all cases, the SSA decay follows a logarithmic equation with three adjustable variables that are parameterized using the initial snow SSA and the time-averaged temperature of the snow. Two parameterizations of the three adjustable variables are found: One applies to the isothermal experiments and to the quasi-isothermal cases studied in Alaska (equitemperature (ET) metamorphism), and the other is applicable to both the laboratory experiments performed under temperature gradients and to the natural snowpack in Alaska (temperature gradient (TG) metamorphism). Higher temperatures accelerate the decrease in SSA, and this decrease is faster under TG than ET conditions. We discuss the conditions of applicability of these parameterizations and use them to speculate on the effect of climate change on snow SSA. Depending on the climate regime, changes in the rate of decay of snow SSA and hence in snow albedo may produce either negative or positive feedbacks on climate change.

**Citation:** Taillandier, A.-S., F. Domine, W. R. Simpson, M. Sturm, and T. A. Douglas (2007), Rate of decrease of the specific surface area of dry snow: Isothermal and temperature gradient conditions, *J. Geophys. Res.*, 112, F03003, doi:10.1029/2006JF000514.

### 1. Introduction

[2] Snow crystals in dry snowpacks are subjected to water vapor gradients generated by temperature gradients in the snowpack and by curvature gradients on the surface of snow crystals. These effects drive sublimation/condensation cycles that modify the sizes and shapes of snow crystals and the physical properties of the snowpack. These changes are grouped under the term “snow metamorphism.” Two main regimes of dry metamorphism are described in the literature [Sommerfeld and LaChapelle, 1970]. Equitemperature (ET) metamorphism takes place under isothermal or low temperature gradient conditions ( $<10^{\circ}\text{C m}^{-1}$ ) and is mostly driven

by curvature gradients. Temperature gradient (TG) metamorphism takes place under temperature gradients greater than  $20^{\circ}\text{C m}^{-1}$  [Marbouty, 1980].

[3] Metamorphism also affects the chemical composition of snow and of the atmosphere above the snow [Domine and Shepson, 2002]. Gases soluble in ice and those that adsorb onto snow crystal surfaces are exchanged with the atmosphere through sublimation/condensation and adsorption/desorption cycles. Adsorbed gases can diffuse inside snow grains and can undergo surface (photo)chemical reactions. Most of these physical and chemical processes involve the surface of snow crystals and their quantification requires the knowledge of the snow surface area, which changes during metamorphism [Cabanes *et al.*, 2002, 2003; Legagneux *et al.*, 2004] and whose variations must be described in models of snow physics and chemistry [Flin *et al.*, 2003; Legagneux and Domine, 2005].

[4] The variable used to describe the surface area available for chemical processes is the specific surface area (SSA), defined as the snow surface area accessible to gases per unit mass, often expressed in  $\text{cm}^2 \text{g}^{-1}$ . Legagneux *et al.* [2002] measured snow SSA values from less than  $100 \text{ cm}^2 \text{g}^{-1}$  for aged snow to  $1580 \text{ cm}^2 \text{g}^{-1}$  for freshly fallen snow. Lei and

<sup>1</sup>Laboratoire de Glaciologie et Géophysique de l'Environnement, CNRS, Saint-Martin d'Hères, France.

<sup>2</sup>Geophysical Institute, University of Alaska Fairbanks, Fairbanks, Alaska, USA.

<sup>3</sup>Department of Chemistry, University of Alaska Fairbanks, Fairbanks, Alaska, USA.

<sup>4</sup>U.S. Army Cold Regions Research and Engineering Laboratory, Fort Wainwright, Alaska, USA.

*Wania* [2004] showed that the snow SSA value is crucial to model organic species scavenging by precipitating snow. *Daly and Wania* [2004] tested the effect of a snow cover on the fate of organic contaminants in the environment using a model that included snow scavenging and the adsorption of organic contaminants to a seasonal snowpack. Calculated wintertime atmospheric concentrations of organic contaminants were low in simulations on the basis of a high snow SSA, while higher concentrations were obtained with a lower SSA. That study demonstrates the importance of snow SSA in models of air-snow chemical interactions. Snow SSA almost always decreases monotonically with time [*Cabanes et al.*, 2002, 2003; *Legagneux et al.*, 2004] and the decay of snow SSA needs to be described in models of air-snow exchange of chemical species if we are to predict events such as spikes of pollutants in air, soil or water during snowmelt [*Daly and Wania*, 2004].

[5] Ice core analyses are used to reconstruct the evolution of atmospheric composition [*Legrand and Mayewski*, 1997]. In the case of adsorbed species [*Villa et al.*, 2003], complex modeling taking into account the reduction of snow SSA with time and the diffusivity of the snow is needed for a precise inversion of ice core data. A quantitative parameterization of the rate of decrease of snow SSA would usefully contribute to such a model.

[6] A quantitative understanding of the rate of decay of snow SSA would also benefit snow physical models. For example, snow albedo depends on grain size [*Warren*, 1982], which can be related to SSA if assumptions on grain shapes are made. *Domine et al.* [2006] have shown the existence of a simple monotonic relationship between snow spectral albedo and SSA, confirming this assertion. Understanding the SSA decay rate of surface snow layers can thus help predict the evolution of the energy budget of a snowpack after a snowfall.

[7] *Cabanes et al.* [2003] first proposed an empirical exponential decay function of snow SSA depending on time and temperature based on the evolution of surface snow layers sampled in the Alps and in the Arctic. They mentioned that other analytical forms could describe snow SSA decay more accurately, but the exponential function was easier to use. *Legagneux et al.* [2003] subsequently performed laboratory experiments under isothermal conditions and observed that SSA decay plots were best fitted using a logarithmic law:

$$SSA(t) = B - A \ln(t + \Delta t) \quad (1)$$

where  $A$ ,  $B$  and  $\Delta t$  are adjustable parameters. Remarkably, they observed that  $A$  and  $B$  were linearly correlated for a given temperature. Although equation (1) provides a simple parameterization of SSA, it is empirical and has its limits. For example SSA values are predicted to become negative after about a year. *Legagneux et al.* [2004] later confirmed equation (1) and interpreted their data within Ostwald ripening theory [*Ostwald*, 1901].

[8] Ostwald ripening describes the coarsening of solid particles with a given size distribution by exchange of matter through a fluid phase, the driving force being the minimization of surface energy. It was treated quantitatively by *Lifshitz and Slyozov* [1961] and *Wagner* [1961], produc-

ing what is known as the LSW theory. *Legagneux et al.* [2004] applied that theory to snow SSA decay during isothermal metamorphism, treating snow crystals as non-connected spheres. They showed that under the LSW theory, snow SSA should follow the rate law:

$$SSA(t) = SSA_0 \left( \frac{\tau}{t + \tau} \right)^{\frac{1}{n}} \quad (2)$$

where  $SSA_0$  is the initial SSA at time  $t = 0$ ,  $n$  is the growth exponent and  $\tau$  is a variable that encompasses the effects of the growth rate and of  $n$ . These authors also showed that equation (1) is in fact an approximation of equation (2), and (1) is valid in the time range from less than 1 day to about 150 days. Using fairly complex equations, they established the relationships between  $A$ ,  $B$  and  $\Delta t$  of equation (1) on the one hand and  $SSA_0$ ,  $\tau$  and  $n$  of equation (2), therefore giving physical meaning to the parameters of equation (1) (see their equations (10) to (13)). They also demonstrated that, although equation (2) fitted SSA decay plots extremely well, the formalism of the LSW theory could not be used to predict SSA decay during isothermal metamorphism because a steady state was not reached in the crystal size distribution within the lifetime of a seasonal snowpack.

[9] In a further attempt to reach a theoretical understanding of snow SSA decay, *Legagneux and Domine* [2005] developed a quantitative model of isothermal snow metamorphism, where exchange of matter between ice spheres of different radii of curvature was caused by the difference in vapor pressure (Kelvin equation). They calculated analytically water vapor transport from the smaller to the larger ice spheres and found that diffusion of water vapor in air was the rate-limiting step. Their model reproduced very accurately the changes in the distribution of radii of curvature of natural snow undergoing isothermal metamorphism, measured by *Flin et al.* [2003] using high-resolution X-ray microtomography. Unfortunately, they were not able to reproduce SSA decay, and interpreted this lack of success by the fact that in real snow, the mass of ice associated with each curvature is different from the value for idealized spheres. Because SSA is the surface area to mass ratio, this caused the error in SSA. They concluded that a more realistic treatment of snow crystal shapes or the use of shape correction factors were necessary to understand SSA decay. Moreover, since natural dry snowpacks are not isothermal, efforts to obtain experimental data under non-isothermal conditions and to develop the corresponding models were recommended.

[10] Recently, *Flanner and Zender* [2006] developed a model (hereinafter referred to as FZ06) of snow SSA decay that treats vapor transport driven by differences in curvature (Kelvin's law) and temperature (Clapeyron's law). Again, the complexity of snow structure caused difficulties. They approximated snow crystals as spheres and used two adjustable parameters,  $\sigma_g$  for the distribution of crystal sizes and  $\phi$  for the irregularity in particle spacing. By adjusting  $\sigma_g$ , they were able to reproduce the experimental isothermal SSA decays of *Legagneux et al.* [2004] with reasonable success, the fit of some decay plots being very good. By adjusting  $\phi$ , they reproduced the data of *Fukuzawa and Akitaya* [1993], who measured the growth in mean diameter

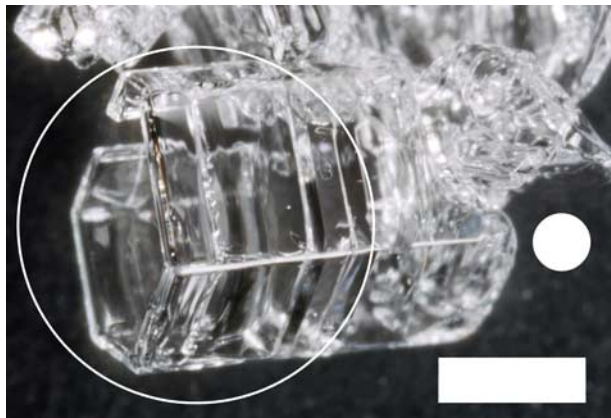


**Figure 1.** Photomicrograph of a depth hoar crystal with  $SSA = 167 \text{ cm}^2 \text{ g}^{-1}$  (see text). The scale bar is 1 mm. The white disc represents an ice sphere of radius  $r_e = 196 \mu\text{m}$  that has a  $SSA$  of  $167 \text{ cm}^2 \text{ g}^{-1}$ . The white circle, of radius 1.20 mm, has the same cross-sectional area as the depth hoar crystal. The  $SSA$  of ice spheres of that radius is  $27 \text{ cm}^2 \text{ g}^{-1}$ .

of crystals growing under temperature gradients of 150 to  $300^\circ\text{C m}^{-1}$ . Here, for the diameters of the crystals, *Flanner and Zender* [2006] used the diameter of spheres with equal cross-sectional areas.

[11] *Fukuzawa and Akitaya* [1993] did not measure  $SSA$  directly, and it is not clear how reliably  $SSA$  can be derived from their data. Indeed, hollow faceted crystals called depth hoar grow under temperature gradients greater than  $20^\circ\text{C m}^{-1}$ . Such a crystal is shown in Figure 1. The snow sample from which this crystal was taken had a  $SSA$  of  $131 \text{ cm}^2 \text{ g}^{-1}$ . The  $SSA$  of this depth hoar crystal can be estimated from its dimensions [*Domine et al.*, 2001]. Briefly, the crystal is approximated by an infinite slab having the same thickness as the walls of the hollow crystal,  $130 \mu\text{m}$ . We find a value of  $167 \text{ cm}^2 \text{ g}^{-1}$ , in good agreement with the value of the whole sample. The radius of the ice sphere with the same  $SSA$  is  $r_e = 3/(\rho_i SSA)$ , where  $\rho_i$  is the density of ice, and here  $r_e = 196 \mu\text{m}$  (note that  $SSA$  is an intensive variable, so that two crystals can have the same  $SSA$  while having different masses). In comparison, the radius of the sphere having the same cross-sectional area as this crystal is 1.20 mm, with a corresponding  $SSA$  of  $27 \text{ cm}^2 \text{ g}^{-1}$  (Figure 1). This example illustrates the potential added error in adjusting a  $SSA$  evolution model with indirect estimations of snow  $SSA$ .

[12] More detailed experimental data of snow  $SSA$  decay under TG conditions are needed. These conditions prevail in the natural snowpack where they are induced by daily and seasonal temperature variations. Such data are critically lacking for the atmospheric chemistry and climate applications mentioned above. FZ06 seems promising in view of its ability to fit the isothermal data of *Legagneux et al.* [2004] but it is not certain that the data of *Fukuzawa and Akitaya* [1993] can be used to test it.

[13] Here, we conduct experiments where snow is subjected to controlled temperature gradients for several months. The snow samples used were collected from the same snow falls and at the same time as those used by

*Legagneux et al.* [2004] for isothermal experiments. This allowed us to compare the evolution of  $SSA$  under ET and TG conditions. During the winter of 2003/2004 we also monitored the  $SSA$  of natural snow layers throughout the winter in Central Alaska, where strong temperature gradients develop in the taiga snowpack [*Sturm and Benson*, 1997; *Taillandier et al.*, 2006]. The taiga snowpack covers large boreal areas. It is sheltered from wind by vegetation and remains of low density, in contrast to the tundra snowpack that is capped by a high-density windpack [*Sturm et al.*, 1995; *Domine et al.*, 2002]. We also monitored the  $SSA$  of these snow layers in Alaska, but modified them so that they evolved under ET conditions.

[14] We then compare our data with predictions by FZ06 and find good agreement. However, FZ06 requires complex numerical modeling. A simpler parameterization may be easier to implement in snowpack models coupled to atmospheric or climate models. We thus propose simple empirical equations that reproduce both ET and TG data and can be readily introduced in models.

## 2. Methods

### 2.1. Isothermal Experiments

[15] Nine snowfalls were collected and subjected to isothermal metamorphism in a cold room. Snow characteristics and experimental conditions were detailed by *Legagneux et al.* [2003, 2004]. Briefly, freshly fallen snow was sampled either in the stainless steel container used to run  $SSA$  measurements or in airtight boxes that were kept in a cold room at the desired temperature ( $-4$ ,  $-10$  or  $-15^\circ\text{C}$ ). Snow  $SSA$  was then measured regularly.

### 2.2. Temperature Gradient Experiments

[16] Two of the snowfalls used for isothermal experiments were also used for temperature gradient experiments. They were sampled during events on 6 March and 2 April 2003 near Chamrousse, in the Belledonne range of the French Alps. The first precipitation event consisted of moderately to heavily rimed plates and dendritic crystals while the second one consisted of graupel. The snow temperature during both events was just below  $0^\circ\text{C}$ . Nine airtight boxes 30 cm high with a basal section  $17 \times 11$  cm were thermally equilibrated with snow and then delicately filled with snow using a 10 cm wide shovel. The boxes were placed in a thermally insulated trunk filled with snow and transported to the laboratory within a half hour. Snow was also sampled into glass vials immediately immersed into liquid nitrogen to measure the  $SSA$  of the freshly fallen snow.

[17] The top and bottom faces of the sampling boxes were made of aluminum while the sides were made of wood. To generate a temperature gradient, the nine boxes tightly packed together were placed in a cold room at  $-15.0^\circ\text{C} \pm 0.1^\circ\text{C}$ , with their base on an aluminum bottom plate heated to  $-5.0^\circ\text{C} \pm 0.2^\circ\text{C}$  (Figure 2). The sides of the boxes were thermally shielded by thick insulating foam. Two fans in the heated space below the heated aluminum plate ensured thermal homogeneity. The inner height of the boxes was 30 cm so the temperature gradient was  $33^\circ\text{C m}^{-1}$ . In one of the boxes, sensors monitored the snow temperature at each sampling level.

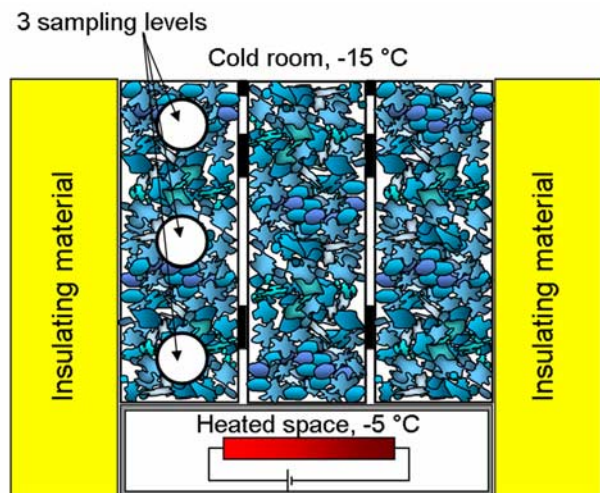


**Figure 2.** Cross section of the experimental thermal gradient apparatus. Three of the nine snow-filled boxes are visible. Boxes are 30 cm in height.

[18] The boxes opened from one side and snow sampling was performed by coring  $130 \text{ cm}^3$  of snow at 3 levels one box at a time (Figure 2) using a metal corer of 35 mm ID. The samples were gently inserted into the cylindrical SSA measurement containers, also 35 mm ID, and the container was immersed in liquid nitrogen. SSA evolution was followed during 102 and 77 days for the snowfalls of 6 March and 2 April 2003, respectively. Since each box was only sampled once, experimental decay plots included

10 data points at the most: those from the nine boxes, plus the measurement of the initial SSA (Figure 3).

**2.3. Field Measurements**

[19] The seasonal Arctic snowpack was studied during winter 2003/2004 at the Large Animal Research Station (LARS), at the University of Alaska Fairbanks ( $64^\circ 52.9'N$ ,  $147^\circ 51.9'W$ ). The natural snowpack investigation was coupled to that of a similar snowpack subjected to very low temperature gradients. This low thermal gradient condition was achieved by letting snow accumulate on large tables ( $1.5 \times 3 \text{ m}$ ) placed 1.5 m above the ground prior to the onset of winter. Air circulation under the tables prevented the establishment of any significant temperature gradient. At this latitude, there is little day light and solar input to the snowpack is limited. Only in March did we observe transient temperature gradients near the snow surface. Probes recorded snow temperature every 7.5 cm inside the natural snowpack and at 3 different heights in the snowpack on one of the tables. Meteorological data (air temperature, wind speed and direction) were continuously monitored on site [Taillandier *et al.*, 2006].

[20] Snow that fell in four separate events was regularly sampled for SSA measurements during the winter (Table 1). Two of these snowfalls were also monitored in the snowpack subjected to low temperature gradient on the tables. The sampling procedure followed Hanot and Domine [1999] and Domine *et al.* [2002]. Briefly, snow pits with vertical faces were dug to observe the stratigraphy and to locate the layers of interest. For each sample, about  $100 \text{ cm}^3$  of snow was collected in a glass vial that was immediately immersed in liquid nitrogen to stop metamorphism until its

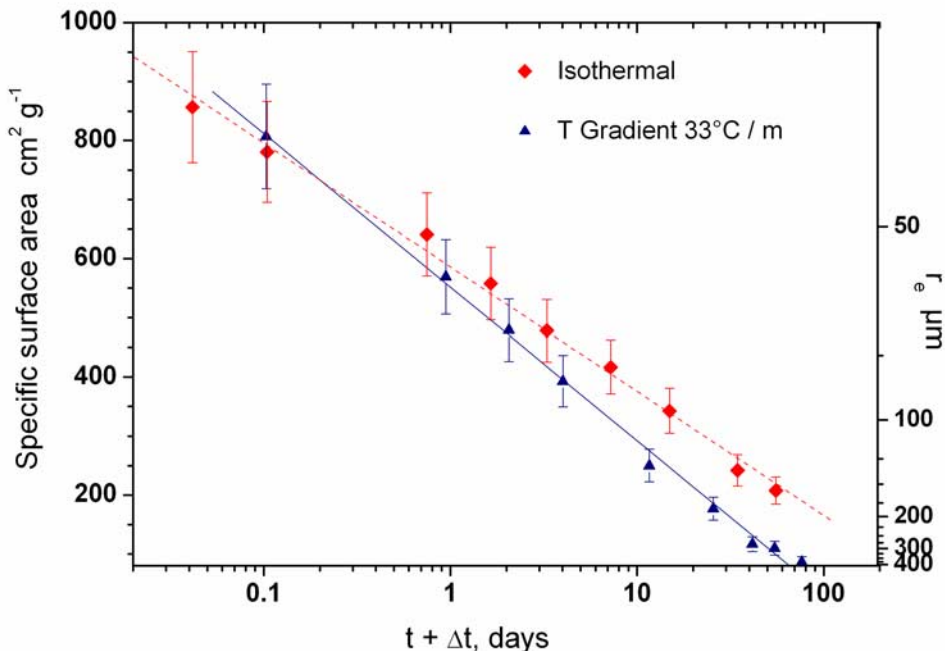


**Figure 3.** SSA decay of the snow layer sampled on 2 April 2003 in the Alps. Isothermal experiment 9 of Table 2 (red diamonds) is compared to temperature gradient experiment 12 (blue triangles). The fits are to equation (1) with coefficients of Table 2. The equivalent sphere radius  $r_e$  is shown on the right ordinate axis.

**Table 1.** Characteristics of the Snowfalls Studied in the Natural Snowpack at the LARS Site, Central Alaska

Date of Snowfall	Initial Snow Density	Final Snow Density	Final Snow Density on Tables <sup>a</sup>	Fresh Snow Crystal Types
10 Nov 2003 <sup>a</sup>	0.10	0.19	0.27	Mostly rimed dendritic crystals
21 Nov 2003	0.08	0.21	-	Lightly rimed dendritic crystals, plates and needles
04 Jan 2004 <sup>a</sup>	0.01	0.20	0.16	Small rimed dendritic crystals
22 Jan 2004	-	0.18	-	Rimed dendritic crystals, capped columns and a few plates

<sup>a</sup>These snowfalls were also monitored in the snowpack subjected to a low temperature gradient on the tables. Snow initial characteristics are the same as in the natural snowpack.

contents were transferred to the SSA measurement container in a cold room at  $-17^{\circ}\text{C}$ . The duration of SSA monitoring under high temperature gradient conditions varied between 29 days for the 22 January 2004 layer and 136 days for the 10 November 2003 layer. On tables, the 10 November 2003 snowfall was monitored for 143 days and the 4 January 2004 snowfall for 88 days.

#### 2.4. Snow-Specific Surface Area Measurements

[21] Snow SSA was determined by measuring the adsorption isotherm of methane on the snow at liquid nitrogen temperature (77 K) using a volumetric method. A mathematical treatment [Brunauer *et al.*, 1938] was used to extract the SSA from the isotherm. The method is detailed by Legagneux *et al.* [2002], who cite a measurement reproducibility of 6% and an accuracy better than 12%. Since that paper, the method was improved by taking into account the adsorption of methane on the stainless steel walls of the experiment container, as alluded to by Legagneux *et al.* [2004] and detailed by Domine *et al.* [2007]. The

reproducibility was unchanged by these modifications, whose main effect was to reduce systematic errors. Methane adsorption on stainless steel was an artifact that was not previously taken into account in our estimate of systematic errors. Given that systematic errors can only be estimated, we still evaluate our current accuracy at 12%.

### 3. Results

#### 3.1. Temperature Gradient Experiments

[22] Boxes containing both snow falls collected near Chamrousse and subjected to gradient metamorphism in a cold room were sampled at 3 levels, corresponding to temperatures roughly of  $-6$ ,  $-10$  and  $-14^{\circ}\text{C}$ , so that 6 SSA decay plots were obtained (Table 2). During sampling, the morphological modifications of the snow crystals were also observed. Qualitatively, from fresh graupel, crystals started to grow and to develop facets after a few days, typical of TG metamorphism. After 20 days, the initial shapes of the snow grains were no longer recognizable and

**Table 2.** Conditions of Evolution of Sampled Snow, Parameters Obtained From Equation (1) and Correlation Coefficients  $R^2$ 

Experiment Number	Snow Layer	Sampling Place	$ \text{grad}(T_m) $ , <sup>a</sup> deg C m <sup>-1</sup>	Mean	Initial Density, g cm <sup>-3</sup>	SSA <sub>0</sub> , <sup>b</sup> cm <sup>2</sup> g <sup>-1</sup>	$A$ , cm <sup>2</sup> g <sup>-1</sup>	$B$ , cm <sup>2</sup> g <sup>-1</sup>	$\Delta t$ , hours	$R^2$	$\Delta t'_{g' or is}$ hours
				Temperature $T_m$ , deg C							
1	16 Jan 2002 <sup>c</sup>	Alps	0	-15	0.075	638	59	674	16	0.979	7.0
2	6 Feb 2002 <sup>c</sup>	Alps	0	-15	0.12	1015	81	820	27	0.997	13.0
3	6 Feb 2002 <sup>c</sup>	Alps	0	-4	0.12	752	72	709	22	0.971	0.5
4	21 Feb 2002 <sup>c</sup>	Alps	0	-15	0.14	551	100	988	-0.25	0.996	1.2
5	21 Feb 2002 <sup>c</sup>	Alps	0	-10	0.18	553	74	722	101	0.975	5.7
6	7 Nov 2002 <sup>c</sup>	Alps	0	-15	0.10	846	85	877	-0.5	0.986	2.3
7	29 Jan 2003	Alps	0	-15	0.05	961	109	1042	1	0.995	1.4
8	6 Mar 2003	Alps	0	-15	0.10	637	74	722	1	0.997	7.1
9	2 Apr 2003	Alps	0	-15	0.15	857	99	921	1	0.998	2.2
	6 Mar 2003	Alps									
10	bottom layer	Alps	33	-6	0.10	637	85	696	0	0.939	1.0
11	middle layer	Alps	33	-10.5	0.10	637	92	756	2	0.976	3.9
12	top layer	Alps	33	-14	0.10	637	115	926	13	0.942	8.4
	2 Apr 2003	Alps									
13	bottom layer	Alps	33	-7	0.15	857	106	849	-0.25	0.969	0.6
14	middle layer	Alps	33	-10.5	0.15	857	109	863	0	0.983	1.5
15	top layer	Alps	33	-14	0.15	857	120	958	1	0.994	3.2
16	10 Nov 2003	Alaska	36	-4.8	0.10	507	57	531	-10.5	0.982	1.3
17	21 Nov 2003	Alaska	31	-6.9	0.08	746	74	644	-0.75	0.990	0.9
18	4 Jan 2004	Alaska	35	-15.5	0.01	885	135	1123	9	0.950	3.8
19	22 Jan 2004	Alaska	54	-15.3	-	527	89	761	-10	0.999	20.5
20	10 Nov 2003	Alaska	8	-19.2	0.10	507	79	778	45	0.989	31.7
21	4 Jan 2004	Alaska	9	-18.4	0.01	885	125	1103	-72	0.995	3.0

<sup>a</sup>The mean absolute value of the temperature gradient  $|\text{grad}(T_m)|$  is calculated between the two buried temperature probes surrounding the layer of interest inside the snowpack.

<sup>b</sup>SSA<sub>0</sub> is the initial specific surface area of the snow sampled right after its fall.

<sup>c</sup>Parameters  $A$ ,  $B$ , and  $\Delta t$  derived from these isothermal experiments differ slightly from those presented by Legagneux *et al.* [2004] because of subsequent minor corrections (see text).

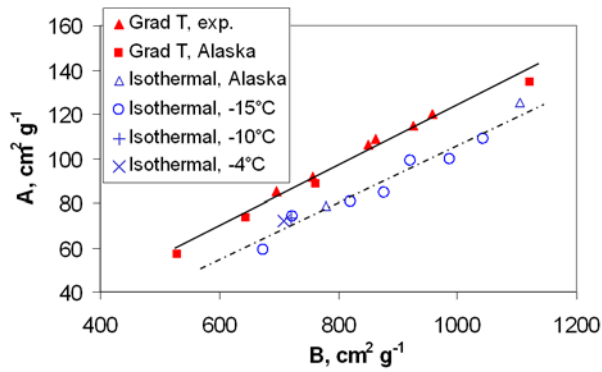


**Figure 4.** Parameters  $A$  versus  $B$  from equation (1). Results from temperature gradient experiments (solid triangles) and from the natural snowpack in Alaska (solid squares) are located on the same line. Data from isothermal experiments at  $-15^{\circ}\text{C}$  [Legagneux et al., 2004] (open circles) are aligned with those at  $-10^{\circ}\text{C}$  (pluses) and  $-4^{\circ}\text{C}$  (crosses) and with those of the quasi-isothermal snowpack of Alaska (open triangles). The solid and dash-dotted lines are least squares fits of the gradient and isothermal data, respectively.

became more and more faceted and elongated, although crystals in the upper (and colder) part of the boxes seemed to be evolving more slowly. Depth hoar crystals started to form after about 2 months and crystal size increased with increasing temperature toward the bottom of the boxes. As in the work by Legagneux et al. [2003], logarithmic ( $\text{SSA} = -A_{\ln} \ln(t) + B_{\ln}$ ), exponential ( $\text{SSA} = B_{\text{exp}} e^{-A_{\text{exp}} t}$ ), power ( $\text{SSA} = B_{\text{power}} t^{-A_{\text{power}}}$ ) and linear laws ( $\text{SSA} = -A_{\text{lin}} t + B_{\text{lin}}$ ) were tested to parameterize the SSA decay rate. The average

correlation coefficients,  $R^2$ , were 0.94, 0.72, 0.90 and 0.51, respectively, showing that the logarithmic fit worked best. This fit was further improved by adding the adjustable parameter  $\Delta t$ , as used by Legagneux et al. [2003] in equation (1).

[23] An example of a SSA decay curve during these gradient experiments is shown in Figure 3 and parameters  $A$ ,  $B$  and  $\Delta t$  are given in Table 2. Legagneux et al. [2003, 2004] observed a linear correlation between  $A$  and  $B$  for snow subjected to isothermal conditions at  $-15^{\circ}\text{C}$  and proposed a theoretical explanation for such a correlation.  $A$  and  $B$  from gradient experiments are plotted in Figure 4, showing that they are aligned, but on a line different from that of the isothermal conditions. We note that these 6 data points are almost perfectly aligned, even though the decays were obtained at 3 different temperatures.

**3.2. Field Measurements of the Natural Snowpack**

[24] The SSA of the four snowfalls studied in the natural snowpack of central Alaska was measured at least five times. The decays were best fitted using equation (1) and an example is given in Figure 5.  $A$  and  $B$  values from these fits are also plotted in Figure 4, showing that the four data points are well aligned. It is reasonable to suggest that the data points from the natural snowpack are on a line parallel to that of the cold room gradient experiments but slightly downshifted. However, we believe that this slight shift is not significant and that it is more meaningful to draw a single line through all the data points obtained under gradient conditions. This shift is probably due to systematic errors. Our volumetric equipment was taken apart and rebuilt after transport to Alaska. Minor modifications took place such as valve and tubing replacements, producing minute changes in their volumes, to which SSA values are extremely sensitive [Legagneux et al., 2002]. Although

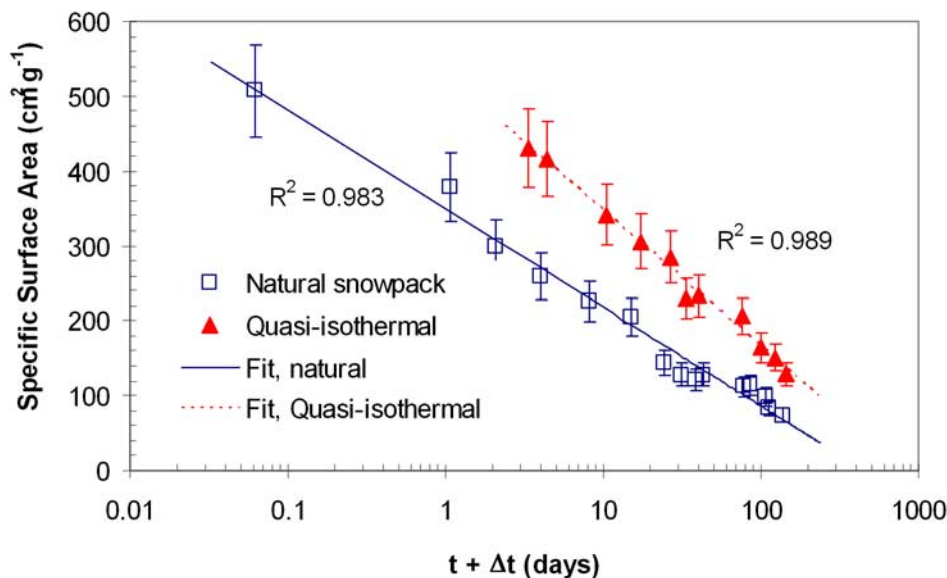


**Figure 5.** Time evolution of the SSA of the snow layer that fell on 10 November 2003 near Fairbanks, Alaska. One decay plot corresponds to the natural snowpack (open squares, experiment 16 in Table 2) that evolved under high-temperature gradients ( $\text{grad}(T)_{\text{mean}} = 36^{\circ}\text{C m}^{-1}$ ), while the other one is of the snow that fell on tables (solid triangles, experiment 20) and evolved under quasi-isothermal conditions (see text). The equivalent sphere radius for a SSA of  $500 \text{ cm}^2 \text{ g}^{-1}$  is  $r_e = 65 \mu\text{m}$ .

great care was taken in volume measurement, very small errors will produce different systematic errors each time the system is rebuilt. We thus suggest that the  $(A, B)$  data points of Figure 4 obtained from cold room experiments and fieldwork in Alaska are actually on a single straight line and that the scatter is due to variations in systematic errors. The least squares equation for this single line is:  $A = 0.135 B - 11.368$  ( $R^2 = 0.982$ ).

### 3.3. Quasi-Isothermal and Isothermal Experiments

[25] Two of the snow layers that accumulated on the Alaska tables were sampled regularly. They also produced logarithmic decay plots and their  $A$  and  $B$  values are reported in Table 2. For comparison, we have also plotted in Figure 4 the  $A$  and  $B$  values obtained by *Legagneux et al.* [2004] from 7 isothermal SSA decay plots at  $-15^\circ\text{C}$ , and from another two plots at  $-10$  and  $-4^\circ\text{C}$ . As in the case of the gradient experiments, all the isothermal and quasi-isothermal  $(A, B)$  values are on a single line. A more careful look indicates that the points are actually on two distinct parallel lines, slightly shifted from each other. Again, this is due to slight changes in the volumes of the experimental system that produced two different lines. (In fact, these data were obtained from 3 distinct states of the experimental system, but two of them resulted in the same systematic errors in Figure 4). The least squares equation of this second line is:  $A = 0.128 B - 21.838$  ( $R^2 = 0.952$ ).

[26] The main conclusion from these results is that all SSA decay plots can be fitted using the logarithmic equation (1). The  $(A, B)$  values are linearly correlated. One correlation exists for SSA decays under TG conditions, and another one for decays under isothermal or quasi-isothermal (i.e., ET) conditions. In both cases, all the  $(A, B)$  points are aligned, regardless of the temperature and the temperature gradient. In the next section, we use these linear correlations to propose an empirical method to predict the rate of SSA decrease of snow that can be used in models. We also test the predictions of FZ06 with our data.

## 4. Discussion

### 4.1. General Objectives

[27] Equations predicting SSA decay are needed to quantify the snow-atmosphere exchange of chemicals [*Domine and Shepson, 2002; Lei and Wania, 2004; Daly and Wania, 2004*], the evolution of snow albedo [*Flanner and Zender, 2006; Domine et al., 2006*] and snow metamorphism in general, since the rate of sublimation/condensation cycles responsible for dry metamorphism include a SSA term [e.g., *Sokratov, 2001*]. From a purely intellectual point of view, a physically based model would be satisfying, and the model of *Flanner and Zender* [2006] is a solid step in that direction. However, given the complexity of snow structure, *Flanner and Zender* [2006] had to make critical approximations, and in particular used nonconnected spherical crystals. Confirming the results of *Legagneux and Domine* [2005], they show that SSA decay rates depend on the distribution of crystal sizes and on the irregularity of particle spacing, two variables that cannot be routinely measured. Therefore, in the end, they used two adjustable parameters,  $\sigma_g$  and  $\varphi$ , to take these variables into account. They obtained  $\sigma_g = 2.3$  from the data of *Legagneux et al.*

[2004] and  $\varphi = 5$  from the data of *Fukuzawa and Akitaya* [1993]. Even with this empirical character, their model is complex and coupling with atmospheric chemistry or climate models increases calculation time. To simplify calculations, *Flanner and Zender* [2006] fit their model results to equation (2),  $\tau$  and  $n$  being determined by standard curve-fitting procedures, and propose to use tables where  $\tau$  and  $n$  are determined from 4 variables: temperature, temperature gradient, density, and  $\text{SSA}_0$ .

[28] *Flanner and Zender* [2006] have confirmed that a fully physically based model of SSA decay would be extremely complex. They have also shown that such a model would require data that barely exist and that will not be routinely measured in the near future. The table based on four variables proposed by *Flanner and Zender* [2006] is a welcome simplification but its use will not always be simple particularly because temperature, temperature gradients and density change continuously during metamorphism. We therefore propose to use the experimental data presented here to simplify the description of the SSA decay rate, and we test below a description as a function of fewer variables, averaged over long time periods.

[29] Our approach is based on the correlation between  $A$  and  $B$  of equation (1) (Figure 4). *Legagneux et al.* [2004] showed that their data under ET conditions were very well described by equation (2), also used by *Flanner and Zender* [2006] and that equation (1) was an approximation of equation (2). Furthermore, *Legagneux et al.* [2004] proposed, from an analysis of LSW equations, an explanation of why  $A$  and  $B$  were linearly correlated, showing that there is more than just an empirical basis to equation (1).

[30] *Legagneux et al.* [2003] observed that the value of  $B$  was close to the SSA of snow collected immediately after its fall,  $\text{SSA}_0$ . They therefore proposed to predict the rate of isothermal decrease of snow SSA from equation (1) with  $B = \text{SSA}_0$  and deriving  $A$  from the  $A$ - $B$  correlation. The value of  $\Delta t$  in equation (1) could not a priori be determined and they proposed to use the time between snowfall and snow sampling as  $\Delta t$ . In any case, the value of  $\Delta t$  was observed to have only a small impact on the fit. For example, for the top layer of the 2 April 03 sampling in the Alps (experiment 15 in Table 2), changing  $\Delta t$  from 1 to 5 hours reduces  $R^2$  from 0.994 to 0.984. For  $\Delta t = 10$  hours, we still have  $R^2 = 0.968$ .

[31] The problem with correlating  $\text{SSA}_0$ ,  $B$  and  $A$  as suggested above is that it assumes that the rate of SSA decrease is temperature-independent, in contrast to the modeling results of *Legagneux and Domine* [2005] and of FZ06. Temperature dependence is expected, as sublimation and condensation rates increase with the water vapor pressure. With the additional data obtained here, we show below that a closer observation of  $\text{SSA}_0$ - $B$ - $A$  correlations allows us to propose temperature-dependent parameterizations of SSA decay rates. On the basis of Figure 4, we distinguish two distinct sets of conditions: TG metamorphism and ET metamorphism, the latter one applying when the temperature gradient is below a given threshold.

### 4.2. Parameterization for Temperature Gradient Conditions

[32] Our purpose is to predict  $A$ ,  $B$  and  $\Delta t$  values, defined in equation (1), knowing  $\text{SSA}_0$ , the initial snow SSA

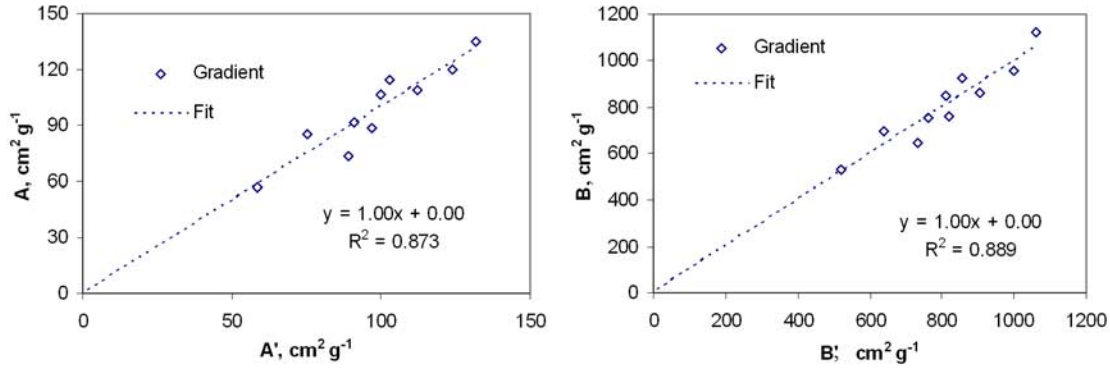


**Figure 6.** Determination of rate parameters for SSA decay under temperature gradient conditions. (left) Least squares fit showing the good agreement between  $A$ , determined experimentally from equation (1), and  $A'_g$ , determined by fitting equation (2). (right) Same but for  $B$  and  $B'_g$ , determined from equations (1) and (3), respectively.

measured just after precipitation, and  $T_m$ , the mean temperature of evolution of the snow layer during the period of interest. Let  $A'_g$ ,  $B'_g$  and  $\Delta t'_g$  be the values of the rate parameters of equation (1) that we want to predict for TG conditions. We want  $A'_g$  and  $B'_g$  to be as close as possible to  $A$  and  $B$  determined from the experiments. Ideally,  $\Delta t'_g$  would be close to  $\Delta t$ , but this is not crucial for reasons detailed above. A careful consideration of the data of Figure 4 and Table 2 indicates that  $A$  and  $B$  values are higher for higher values of  $SSA_0$  and for lower mean temperatures of evolution of the snow,  $T_m$ . Hence we propose to test whether it is possible to determine  $A'_g$  and  $B'_g$  using equations (3) and (4):

$$A'_g = a_g SSA_0 - b_g (T_m + c_g) \quad (3)$$

$$B'_g = x_g SSA_0 - y_g (T_m + z_g) \quad (4)$$

An extra constraint on the predicted parameters is that at the time of snow sampling, ( $t = 0$ ) we must have  $SSA = SSA_0$ , in other words  $SSA_0 = B'_g - A'_g \ln(\Delta t'_g)$ , i.e.,

$$\Delta t'_g = e^{\frac{B'_g - SSA_0}{A'_g}} \quad (5)$$

We adjusted  $a_g$ ,  $b_g$ ,  $c_g$ ,  $x_g$ ,  $y_g$ ,  $z_g$  in order to minimize the difference between  $A$  and  $A'_g$  and between  $B$  and  $B'_g$ . This was done by plotting  $A$  as a function of  $A'_g$  and adjusting  $a_g$ ,  $b_g$  and  $c_g$  to maximize the correlation coefficient, while maintaining a slope of 1 and an intercept of 0. The same was done for  $B$  and  $B'_g$  and  $x_g$ ,  $y_g$  and  $z_g$ . We obtained with  $A'_g$ ,  $B'_g$  and  $SSA_0$  in  $\text{cm}^2 \text{g}^{-1}$ ,  $T_m$  in  $^\circ\text{C}$ , and  $\Delta t'_g$  in hours:

$$A'_g = 0.0961 SSA_0 - 3.44(T_m + 1.90) \quad (6)$$

$$B'_g = 0.659 SSA_0 - 27.2(T_m - 2.03) \quad (7)$$

$$\Delta t'_g = e^{\left[ \frac{-0.341 SSA_0 - 27.2(T_m - 2.03)}{0.0961 SSA_0 - 3.44(T_m + 1.90)} \right]} \quad (8)$$

Figure 6 compares  $A$  and  $A'_g$ , and  $B$  and  $B'_g$ . The comparison between  $\Delta t$  and  $\Delta t'_g$  can be seen in Table 2. From expressions (6) and (7), the evolution of snow SSA under gradient conditions is, again with  $t$  in hours,  $T_m$  in  $^\circ\text{C}$  and  $SSA_0$  and  $SSA_g(t)$  in  $\text{cm}^2 \text{g}^{-1}$ :

$$SSA_g(t) = [0.659 SSA_0 - 27.2(T_m - 2.03)] - [0.0961 SSA_0 - 3.44(T_m + 1.90)] \cdot \ln \left\{ t + e^{\left[ \frac{-0.341 SSA_0 - 27.2(T_m - 2.03)}{0.0961 SSA_0 - 3.44(T_m + 1.90)} \right]} \right\} \quad (9)$$

Uncertainties on the coefficients were found to be less than 3% by propagating random errors of 6% (the reproducibility of a SSA measurement) on individual SSA measurements. We found that random propagation in a given decay plot produced changes in experimental ( $A$ ,  $B$ ) values of less than 4% and less than 8 h on  $\Delta t$ . The determination of  $A'_g$ ,  $B'_g$  and  $\Delta t'_g$  takes into account 10  $A$ ,  $B$  and  $\Delta t$  values, resulting in fluctuation damping and in small errors.

#### 4.3. Parameterization for Quasi-Isothermal Conditions

[33] The same procedure was used to determine the predicted values of the rate parameters under ET conditions,  $A'_i$  and  $B'_i$  (Figure 7). The results are

$$A'_i = 0.0760 SSA_0 - 1.76(T_m - 2.96) \quad (10)$$

$$B'_i = 0.629 SSA_0 - 15.0(T_m - 11.2) \quad (11)$$

$$\Delta t'_i = e^{\left[ \frac{-0.371 SSA_0 - 15.0(T_m - 11.2)}{0.0760 SSA_0 - 1.76(T_m - 2.96)} \right]} \quad (12)$$

The rate expression for the evolution of SSA under isothermal conditions is then, again with  $t$  in hours,  $T_m$  in  $^\circ\text{C}$  and  $SSA_0$  and  $SSA_i(t)$  in  $\text{cm}^2 \text{g}^{-1}$ :

$$SSA_i(t) = [0.629 SSA_0 - 15.0(T_m - 11.2)] - [0.0760 SSA_0 - 1.76(T_m - 2.96)] \cdot \ln \left\{ t + e^{\left[ \frac{-0.371 SSA_0 - 15.0(T_m - 11.2)}{0.0760 SSA_0 - 1.76(T_m - 2.96)} \right]} \right\} \quad (13)$$

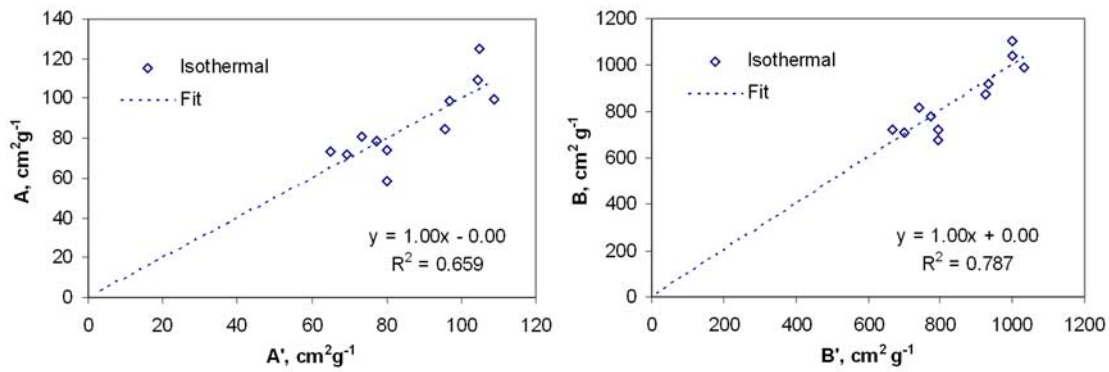


Figure 7. Same as Figure 6 but for SSA decay under isothermal conditions.

As for equation (9), uncertainties on the coefficients were found to be less than 3%.

4.4. Data-Model Comparisons

[34] Before discussing the conditions of validity of equations (9) and (13), it is necessary to compare their predictions to our experimental data. At the same time, we also test the predictions of FZ06, using equation (2), which gives an excellent approximation of the output of FZ06, using values of  $\tau$  and  $n$  kindly supplied by *Flanner and Zender* [2006].

[35] Figure 8 compares four experimental SSA decay plots with predictions from equation (9) or (13) and of

FZ06. Equations (9) and (13) reproduce all decay plots well, as expected because the adjustable parameters of these equations were fitted with those data. This agreement is nevertheless required to justify our explicit and implicit assumptions: (1) there are two distinct metamorphic regimes; (2) snow density is not a critical variable; (3) the value of the temperature gradient is not important within each regime; (4) the mean temperature of evolution is an acceptable substitute to the detailed temperature history. These aspects are discussed in more detail in subsequent paragraphs. Less expected is that FZ06 reproduces our data well in most cases. Indeed, FZ06 was tested by its authors

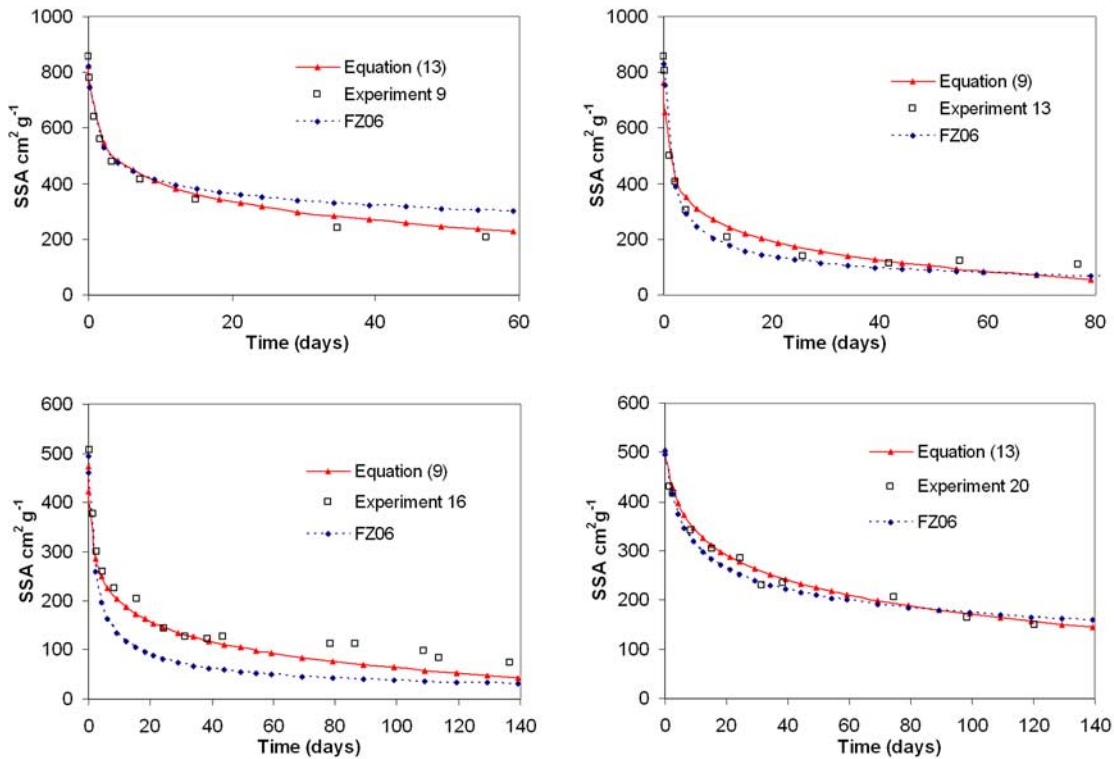


Figure 8. Comparison of the experimental data with the predictions of equation (13) for quasi-isothermal SSA decays 9 and 20 of Table 2 and with the predictions of equation (9) for SSA decays 13 and 16 under temperature gradient conditions. The predictions of model FZ06 for the snow densities, temperatures, and temperature gradients of Table 2 are also shown (see text).

under TG conditions with the data of *Fukuzawa and Akitaya* [1993] and in view of the nature of these data, it was not certain that it would fit actual SSA data well. The fit for experiment (13) is good, in fact as good as equation (9). Experiment (20) also shows an excellent fit. Experiment (16), although still good, is not fitted quite as well as the others. These runs of FZ06 were done without prior adjustments of  $\sigma_g$  and  $\varphi$ : respective values of 2.3 and 5 were used as recommended by *Flanner and Zender* [2006]. It would probably be possible to improve the fits by adjusting  $\sigma_g$  and  $\varphi$ , but we wanted to test the predictive value of FZ06. We conclude that it is in general quite good. We now discuss the conditions of validity of equations (9) and (13), commenting whenever relevant on the expected performance of FZ06 under the same conditions.

#### 4.5. Conditions of Validity of the Rate Equations

[36] Empirical relationships are generally valid only in the range of values investigated experimentally. In particular, equations (1), (9) and (13) are not valid at long times, because SSA values must remain positive. *Legagneux et al.* [2004] showed (their Figure 4) that in the isothermal case, equation (1) is a satisfactory approximation of the more accurate Ostwald ripening equation in the time range 0.5 to about 150 days. At short evolution times, equation (1) is valid only when  $(t + \Delta t) > 1$ , as  $SSA_0 > SSA(t)$ . The validity at long evolution times, estimated from our data, appears to be about 150 days in the ET case. This is adequate for most applications to seasonal snowpacks. In the TG case, depth hoar crystals form and SSA seems to trend asymptotically to about  $80 \text{ cm}^2 \text{ g}^{-1}$  ( $r_e = 409 \text{ }\mu\text{m}$ ). The validity of equation (9) is then about 100 days. Beyond that, taking a constant value of about  $80 \text{ cm}^2 \text{ g}^{-1}$  appears adequate.

[37] That the SSA of depth hoar reaches an asymptotic nonzero value is explained by the crystal shape (Figure 1). Observed growth is essentially along the axis of the hollow prism. To a first approximation [*Domine et al.*, 2001], the SSA of sufficiently large crystals will then be that of an infinite ice slab of the same thickness as that of the hollow prisms. This asymptotic value is not predicted by FZ06, which treats crystals as indefinitely growing spheres. However, Figure 8 shows that for durations relevant to seasonal snowpacks, this aspect does not cause major errors in the predictions of FZ06.

[38] Figure 4 indicates that there are two regimes of SSA decay rate: ET and TG conditions, that correspond to the domains of predominance of two physical processes: curvature-driven metamorphism in the ET case [*Colbeck*, 1980; *Flin et al.*, 2003; *Domine et al.*, 2003; *Legagneux et al.*, 2004] and temperature gradient-driven metamorphism in the other case [*Marbouty*, 1980; *Colbeck*, 1983; *Domine et al.*, 2003]. Table 2 suggests that there may be an abrupt transition between both processes, as the mean temperature gradient for the ET evolution in Alaska was  $8 \text{ to } 9^\circ\text{C m}^{-1}$ . *Marbouty* [1980] suggested that  $20^\circ\text{C m}^{-1}$  was the threshold gradient for depth hoar formation, so that the boundary between ET and TG conditions, as far as SSA decay is concerned, lies somewhere between  $9 \text{ and } 20^\circ\text{C m}^{-1}$ .

[39] This observation seems to contradict *Colbeck* [1982] who stated that “radius of curvature differences cannot control the rate of metamorphism except possibly for brief

periods immediately following a snowfall, when dendrite branches with a mean radius of  $10^{-3} \text{ mm}$  might occur”. Here we suggest that as long as the temperature gradient is below a given threshold, ET metamorphism will control the rate of SSA decrease. This disagreement may only be apparent, however, as *Colbeck* was concerned with grain size and aspect, while we discuss SSA. *Flanner and Zender* [2006] also clearly show that ET metamorphism has a significant effect on SSA decay rate. Their Figure 5 demonstrates that under ET conditions, The SSA decay rate is only about half of that under  $TG = 50^\circ\text{C m}^{-1}$ .

[40] In the ET case, the  $T_m$  range studied is fairly narrow, from  $-19.2 \text{ to } -4^\circ\text{C}$ , and one may wonder whether equation (13) applies beyond that range. Arguments supporting that it does include (1) the snow layers studied in Alaska were subjected to temperatures ranging from  $-43^\circ\text{C}$  to  $0^\circ\text{C}$ ; (2) *Legagneux et al.* [2004] give theoretical support for the (A, B) correlation that is a priori valid at all temperatures. Of course, these considerations do not constitute a proof and additional data at low temperatures are desirable. However, we feel that extrapolating equation (13) below  $-19.2^\circ\text{C}$  is reasonable.

[41] The situation is more complex in the TG case. An extra variable is the magnitude of the temperature gradient. Water vapor fluxes depend on this magnitude and intuitively, one would expect the rate of SSA decay to depend on this variable. From Table 2, the range of mean temperature gradients studied is only from  $31 \text{ to } 54^\circ\text{C m}^{-1}$ . Within this range, we detect no effect of the magnitude of the temperature gradient on SSA decay rate. However, the above values are averages over long time periods and gradient values as high as  $198^\circ\text{C m}^{-1}$  were encountered at the beginning of the season of the Alaska field study. This leads us to suggest that the magnitude of the temperature gradient, as long as it is above a certain threshold, may not have a significant effect on SSA decay rate. This may seem counterintuitive, but one should not confuse metamorphic rate and SSA decay rate. A possible explanation is that microscopic details such as the thickness of the walls of depth hoar crystals determine SSA, rather than macroscopic characteristics such as visual crystal size. While crystal size is likely affected by the temperature gradient, it is possible that microscopic details are less affected. It may then be reasonable to suggest that equation (9) may apply over the whole range of temperature gradients observed in snowpacks. FZ06 predicts an effect of the magnitude of the temperature gradient, but this is expected since they approximate crystals as spheres. Spheres will then grow more rapidly under higher gradients and SSA will decay faster. Models with more realistic crystal shapes are needed to better understand the impact of the temperature gradient on SSA decay rates.

[42] Other variables such as density should also affect the SSA decay rate, as indicated by the models of *Legagneux and Domine* [2005] and by FZ06. Density certainly has an effect, but Table 2 shows that our experimental density range is narrow, with all values  $< 0.18 \text{ g cm}^{-3}$ . One value was very low:  $0.01 \text{ g cm}^{-3}$ , but these low values always lead to very rapid compaction so their effect is very time limited. We therefore think that density effects, if they exist, were too small to be detected by our measurements. Similarly, *Marbouty* [1980] could not detect density effects

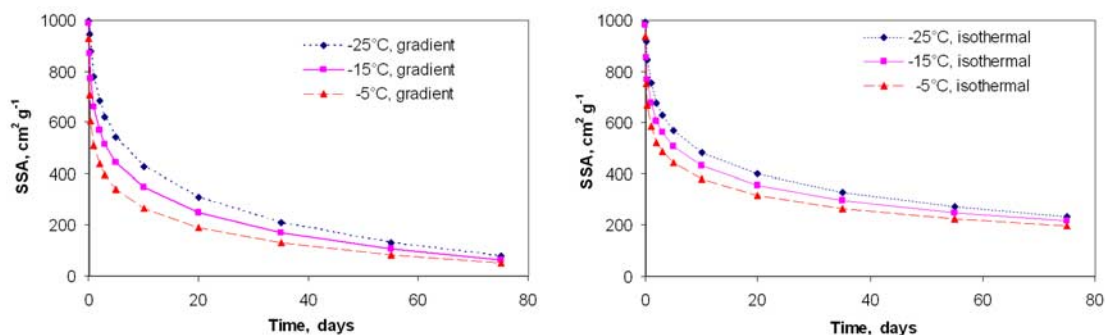


**Figure 9.** Effect of temperature on the rate of SSA decrease for snow having an initial SSA of  $1000 \text{ cm}^2 \text{ g}^{-1}$ , i.e., with  $r_e = 33 \text{ }\mu\text{m}$ . Time plots at  $-25^\circ\text{C}$ ,  $-15^\circ\text{C}$ , and  $-5^\circ\text{C}$  are shown (left) under temperature gradient (TG) conditions and (right) under isothermal (ET) conditions.

in his crystal growth rates for low-density snows ( $<0.15 \text{ g cm}^{-3}$ ). We cannot, however, exclude the possibility that higher densities would have a detectable effect. In fact, two measurements two months apart of the SSA of an identified windpack of density  $0.48 \text{ g cm}^{-3}$  evolving under ET conditions in the high Arctic show that its SSA had only decreased from  $160$  to  $150 \text{ cm}^2 \text{ g}^{-1}$  [Domine et al., 2002]. This slow decrease in high-density windpacks was predicted by Flanner and Zender [2006], which does suggest that SSA decays much slower in high-density snow. In that case, equation (13) would not apply to very dense snow such as Arctic windpacks.

[43] The permeability and diffusivity of snow, by modifying water vapor transfer rates, may also modify SSA decay rates. Snow permeability was measured in Alaska, as will be detailed in a subsequent publication. Values between  $40$  and  $650 \times 10^{-10} \text{ m}^2$  were found, but no correlation between permeability and SSA decay rate was observed. Moreover, permeability increased several fold during the evolution of a given snowfall under TG conditions and this had no detectable effect on SSA decay plots. Possibly this is for reasons similar to those invoked to explain why the magnitude of the temperature gradient plays no obvious role: the microstructure of snow crystals is what actually determines SSA, rather than parameters such as crystal size or crystal growth rates.

[44] Last, our equations were obtained studying the evolution of fresh snow under ET and TG conditions and may not apply to the evolution of aged snow. For example the TG metamorphism of melt-freeze layers formed in the fall may in fact result in a SSA increase.

[45] To conclude this section, we suggest that equations (9) and (13) apply under wide ranges of temperature and temperature gradient. We see no experimental indication that snow permeability, within the range of values studied, affects SSA decay rates. The main limitation to our equations is the density range: our fresh snows had densities  $<0.18 \text{ g cm}^{-3}$  and density never increased beyond  $0.28 \text{ g cm}^{-3}$ . Windpack measurements under ET conditions [Domine et al. 2002] and FZ06 predictions under TG conditions indicate that SSA decay is slower in high-density snows. We therefore recommend to use equations (9) and (13) only for low- to medium-density snows,  $<0.30 \text{ g cm}^{-3}$ , as found in the Alpine and taiga snowpack types. We recommend

further measurements of the SSA evolution of dense snows such as Arctic windpacks.

#### 4.6. Temperature Dependence of SSA Decay Rates

[46] The temperature derivatives of equations (9) and (13) have a complex form that does not lend itself to simple discussions. It is easier to show Figure 9, which plots the SSA decrease of snow with  $\text{SSA}_0 = 1000 \text{ cm}^2 \text{ g}^{-1}$ . As expected, SSA remains lower at all evolution times when temperature is higher. Figure 9 shows that the rate of decrease is more sensitive to temperature when a gradient is present.

#### 4.7. Climate Change and Snow SSA

[47] A legitimate question is how climate change will affect snow SSA. As detailed in the introduction, this is important to predict how air-snow exchange of chemical species will be modified by climate change. However, it will also affect physical variables such as albedo that determine the energy budget of the surface. Climate change-induced modifications of snow SSA may then result in climate feedbacks.

[48] Climate change will affect many physical variables that affect snow SSA. These include temperature but also (1) the amount of precipitation, which impacts the temperature gradient; (2) the wind speed, which affects snow density; and (3) the frequency of precipitation events, which affects the age of the surface snow layer. Extensive discussion of the climate change–snow SSA interactions is not within our current capabilities but we wish to motivate investigations of these interactions by detailing a few selected cases.

[49] Figure 9 shows that warming will result in a lower snow SSA. Hence snow albedo, which decreases with increasing grain size [Warren, 1982] and with decreasing SSA [Domine et al., 2006], decreases with climate warming. If all other variables remained equal this would produce a positive feedback on warming.

[50] The other two climate change-induced modifications discussed here are: (1) an increase in precipitation without significant warming and (2) an increase in precipitation concomitant with warming. In case 1, the increased precipitation will reduce the temperature gradient in the snowpack and in some cases, may take it below the ET/TG threshold, so that equation (13) rather than equation (9) will apply.

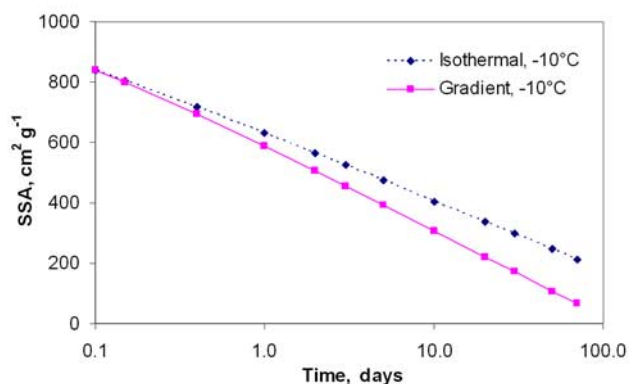


**Figure 10.** Effect of a modification in metamorphic regime, from gradient (TG) to isothermal (ET), on the rate of decrease of snow SSA (with an initial snow SSA of  $1000 \text{ cm}^2 \text{ g}^{-1}$ ). This modification can be caused by an increase in precipitation induced by a change in climate and results in a slower decrease of snow SSA. On this graph, because of the logarithmic scale and because SSA is plotted against  $t$  instead of  $(t + \Delta t)$ , the curves do not start at  $\text{SSA}_0 = 1000 \text{ cm}^2 \text{ g}^{-1}$ .

Figure 10 shows that in this case, the rate of decrease of snow SSA will be slower. The reduction in temperature gradient because of increased precipitation, through its effect on albedo, will then enhance surface cooling. Figure 10 shows results at  $-10^\circ\text{C}$ , but the conclusion is the same regardless of the temperature. As a consequence, increasing precipitation rates, without changes in other variables, acts to increase snow albedo and cause cooling if the threshold between the TG and the ET regimes is crossed.

[51] In case 2, we again make the hypothesis that the increase in precipitation produces a change from the TG to the ET metamorphic regimes. The SSA decay rate is then subjected to two opposite effects: the warmer temperature increases it while the change in regime decreases it. Figure 11 shows the net result, if the temperature warms from  $-10$  to  $-6^\circ\text{C}$ . After less than a day, the snow SSA is greater after climate change than before, so that if a given snow layer is not covered by the subsequent snowfall within about 2 days, a negative feedback related to snow albedo is produced. For a warming of  $4^\circ\text{C}$ , similar results are obtained at all temperatures: we observe that after an initial period where snow SSA is lower under warmer conditions, the curves cross and snow SSA is then higher in the isothermal and warmer snowpack. The crossover time is less than 0.1 day if the temperature is  $-4^\circ\text{C}$  before warming, 3.5 days if it is  $-20^\circ\text{C}$  and 9 days if it is  $-35^\circ\text{C}$ . We then speculate that in some areas where warming will be accompanied by a change in metamorphic regime, the change in the rate of snow SSA decrease may produce a negative feedback on warming.

[52] To conclude this section, we stress that climate change–snow SSA interactions are complex but deserve consideration when modeling climate change in snow covered areas. Most snow-climate feedbacks discussed so far are related to the reduced areal coverage of snow [Dye, 2002] and to increased light absorption by the snow due to

enhanced soot deposition [Jacobson, 2004]. These feedbacks are positive. While we mention extra positive feedbacks such as the enhanced decay rate of SSA caused by warming, we stress that negative feedbacks may take place and need to be quantified to accurately predict climate change.

#### 4.8. Final Remarks

[53] The main result from this work is that both under ET and TG conditions the SSA decay rate obeys equation (1). Adjustable parameters  $A$  and  $B$  are linearly correlated and two distinct correlations are found for the ET and TG conditions. We suggest that this is due to two different processes being the driving forces under each condition. The threshold between both regimes is found to be for a temperature gradient somewhere between  $9$  and  $20^\circ\text{C m}^{-1}$ . We propose and verify empirically that  $A$ ,  $B$  and  $\Delta t$  values can be accurately predicted using the SSA value of the snow right after its fall,  $\text{SSA}_0$ , and the mean temperature of evolution of the snow layer  $T_m$ . We thus obtain rate equations (9) and (13) that predict snow SSA as a function of time and mean temperature, for TG and ET conditions. These equations predict that SSA decay rates increase with increasing temperature and this increase is greater under TG conditions. We discuss the conditions of applicability of equations (9) and (13) and conclude that they should apply over a wide range of temperature and temperature gradient values. The main limitation to these equations is that they may not apply for snow densities greater than  $0.30 \text{ g cm}^{-3}$  and we recommend further measurements of SSA decay in high-density snow. We thus hope that equations (9) and (13) can soon be applied to model atmosphere–snow chemical exchanges and snow physical processes.

[54] The SSA of recently fallen snow,  $\text{SSA}_0$ , is necessary to calculate the coefficients of equations (9) and (13). Until we understand the factors that determine  $\text{SSA}_0$ , we recommend using mean values from the compilations of Legagneux *et al.* [2002] and Domine *et al.* [2007]. For dendritic crystals, unrimed to heavily rimed, the recom-

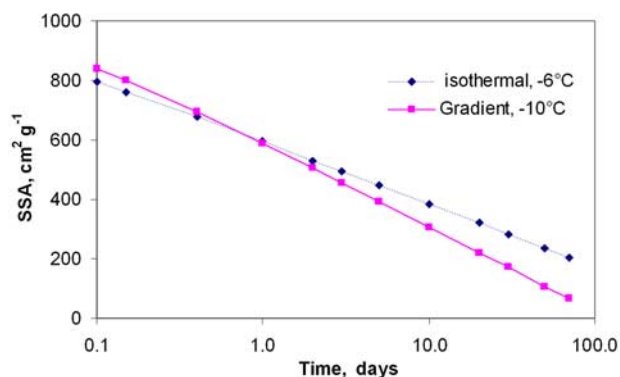


**Figure 11.** Effect of a modification in metamorphic regime combined with a warming of  $4^\circ\text{C}$  on the rate of decrease of snow SSA (with an initial snow SSA of  $1000 \text{ cm}^2 \text{ g}^{-1}$ ). After less than 1 day, snow SSA will be higher in a warmer climate. On this graph, because of the logarithmic scale and because SSA is plotted against  $t$  instead of  $(t + \Delta t)$ , the curves do not start at  $\text{SSA}_0 = 1000 \text{ cm}^2 \text{ g}^{-1}$ .

mended value is  $849 \text{ cm}^2 \text{ g}^{-1}$  ( $r_e = 39 \text{ }\mu\text{m}$ ). For small columns and bullet combinations the value is  $809 \text{ cm}^2 \text{ g}^{-1}$  ( $r_e = 40 \text{ }\mu\text{m}$ ). For small plates, needles and columns, the value is  $658 \text{ cm}^2 \text{ g}^{-1}$  ( $r_e = 50 \text{ }\mu\text{m}$ ) and for snow falling when the ground air temperature is  $>0^\circ\text{C}$ , the value is  $503 \text{ cm}^2 \text{ g}^{-1}$  ( $r_e = 65 \text{ }\mu\text{m}$ ). Predicting  $\text{SSA}_0$  will be complex because it is determined by snow microstructure. We speculate that it could be predicted by complex modeling of crystal growth using physical and chemical variables within and below the cloud, including the concentration of ice nuclei, the supersaturation and temperature within the cloud, the cloud cooling rate and the temperature and humidity profiles between the cloud and the ground.

[55] **Acknowledgments.** The experimental work was performed in France and was funded by CNRS through Programme National de Chimie Atmosphérique. The Alaska fieldwork was partially supported by Chapman Chair funds, kindly supplied by Norbert Untersteiner. A.S.T. and F.D. thank the Geophysical Institute, University of Alaska Fairbanks, for hosting them during the fieldwork, while they were supported by CNRS and the French Ministry of Research. Additional funds were supplied by the International Arctic Research Center to partially support A.S.T. We all extend our warmest thanks to Bill Hauer and his staff for proposing the LARS site for this study and for doing whatever was possible to facilitate our fieldwork. Hajo Eicken is gratefully thanked for the use of the cold rooms at the Geophysical Institute. Mark Flanner kindly supplied the  $n$  and  $\tau$  values used in Figure 8. Comments by two anonymous reviewers and by Steve Warren were helpful in improving initial versions of this paper.

## References

- Brunauer, S., P. H. Emmet, and E. Teller (1938), Adsorption of gases in multimolecular layers, *J. Am. Chem. Soc.*, *60*, 309–319.
- Cabanes, A., L. Legagneux, and F. Domine (2002), Evolution of the specific surface area and of crystal morphology of Arctic fresh snow during the ALERT 2000 campaign, *Atmos. Environ.*, *36*, 2767–2777.
- Cabanes, A., L. Legagneux, and F. Domine (2003), Rate of evolution of the specific surface area of surface snow layers, *Environ. Sci. Technol.*, *37*, 661–666.
- Colbeck, S. C. (1980), Thermodynamics of snow metamorphism due to variations in curvature, *J. Glaciol.*, *26*, 291–301.
- Colbeck, S. C. (1982), An overview of seasonal snow metamorphism, *Rev. Geophys.*, *20*, 45–61.
- Colbeck, S. C. (1983), Theory of metamorphism of dry snow, *J. Geophys. Res.*, *88*, 5475–5482.
- Daly, G. L., and F. Wania (2004), Simulating the influence of snow on the fate of organic compounds, *Environ. Sci. Technol.*, *38*, 4176–4186.
- Domine, F., and P. B. Shepson (2002), Air-snow interactions and atmospheric chemistry, *Science*, *297*, 1506–1510.
- Domine, F., A. Cabanes, A.-S. Taillandier, and L. Legagneux (2001), Specific surface area of snow samples determined by  $\text{CH}_4$  adsorption at 77 K, and estimated by optical microscopy and scanning electron microscopy, *Environ. Sci. Technol.*, *35*, 771–780.
- Domine, F., A. Cabanes, and L. Legagneux (2002), Structure, microphysics, and surface area of the Arctic snowpack near Alert during ALERT 2000 campaign, *Atmos. Environ.*, *36*, 2753–2765.
- Domine, F., T. Lauzier, A. Cabanes, L. Legagneux, W. F. Kuhs, K. Techmer, and T. Heinrichs (2003), Snow metamorphism as revealed by scanning electron microscopy, *Microsc. Res. Tech.*, *62*, 33–48.
- Domine, F., R. Salvatori, L. Legagneux, R. Salzano, M. Fily, and R. Casacchia (2006), Correlation between the specific surface area and the short wave infrared (SWIR) reflectance of snow: Preliminary investigation, *Cold Reg. Sci. Technol.*, *46*, 60–68, doi:10.1016/j.coldregions.2006.06.002.
- Domine, F., A.-S. Taillandier, and W. R. Simpson (2007), A parameterization of the specific surface area of seasonal snow for field use and for models of snowpack evolution, *J. Geophys. Res.*, *112*, F02031, doi:10.1029/2006JF000512.
- Dye, D. G. (2002), Variability and trends in the annual snow-cover cycle in northern hemisphere land areas, 1972–2000, *Hydrol. Processes*, *16*, 3065–3077.
- Flanner, M. G., and C. S. Zender (2006), Linking snowpack microphysics and albedo evolution, *J. Geophys. Res.*, *111*, D12208, doi:10.1029/2005JD006834.
- Flin, F., J.-B. Brzoska, B. Lesaffre, C. Coleou, and R. A. Pieritz (2003), Full three-dimensional modelling of curvature-dependent snow metamorphism: First results and comparison with experimental tomographic data, *J. Phys. D Appl. Phys.*, *36*, 1–6.
- Fukuzawa, T., and E. Akitaya (1993), Depth hoar crystal growth in the surface layer under high temperature gradient, *Ann. Glaciol.*, *19*, 39–45.
- Hanot, L., and F. Domine (1999), Evolution of the surface area of a snow layer, *Environ. Sci. Technol.*, *33*, 4250–4255.
- Jacobson, M. Z. (2004), Climate response of fossil fuel and biofuel soot, accounting for soot's feedback to snow and sea ice albedo and emissivity, *J. Geophys. Res.*, *109*, D21201, doi:10.1029/2004JD004945.
- Legagneux, L., and F. Domine (2005), A mean field model of the decrease of the specific surface area of dry snow during isothermal metamorphism, *J. Geophys. Res.*, *110*, F04011, doi:10.1029/2004JF000181.
- Legagneux, L., A. Cabanes, and F. Domine (2002), Measurement of the specific surface area of 176 snow samples using methane adsorption at 77 K, *J. Geophys. Res.*, *107*(D17), 4335, doi:10.1029/2001JD001016.
- Legagneux, L., T. Lauzier, F. Domine, W. F. Kuhs, T. Heinrichs, and K. Techmer (2003), Rate of decay of specific surface area of snow during isothermal experiments and morphological changes studied by scanning electron microscopy, *Can. J. Phys.*, *81*, 459–468.
- Legagneux, L., A.-S. Taillandier, and F. Domine (2004), Grain growth theories and the isothermal evolution of the specific surface area of snow, *J. Appl. Phys.*, *95*, 6175–6184.
- Legrand, M., and P. Mayewski (1997), Glaciochemistry of polar ice cores: A review, *Rev. Geophys.*, *35*, 219–243.
- Lei, Y. D., and F. Wania (2004), Is rain or snow a more efficient scavenger of organic chemicals?, *Atmos. Environ.*, *38*, 3557–3571.
- Lifshitz, I. M., and V. V. Slyozov (1961), The kinetics of precipitation from supersaturated solid solutions, *J. Phys. Chem. Solids*, *19*, 35–50.
- Marbouty, D. (1980), An experimental study of temperature-gradient metamorphism, *J. Glaciol.*, *26*, 303–312.
- Ostwald, W. (1901), *Analytische Chemie*, 3rd ed., Engelmann, Leipzig, Germany.
- Sokratov, S. A. (2001), Parameters influencing the recrystallization rate of snow, *Cold Reg. Sci. Technol.*, *33*, 263–274.
- Sommerfeld, R. A., and E. LaChapelle (1970), The classification of snow metamorphism, *J. Glaciol.*, *9*, 3–17.
- Sturm, M., and C. S. Benson (1997), Vapor transport, grain growth and depth-hoar development in the subarctic snow, *J. Glaciol.*, *43*, 42–59.
- Sturm, M., and J. B. Johnson (1991), Natural convection in the subarctic snow cover, *J. Geophys. Res.*, *96*, 11,657–11,671.
- Sturm, M., J. Holmgren, and G. E. Liston (1995), A seasonal snow cover classification system for local to global applications, *J. Clim.*, *8*, 1261–1283.
- Taillandier, A.-S., F. Domine, W. R. Simpson, M. Sturm, T. A. Douglas, and K. Severin (2006), Evolution of the snow area index (SAI) of the subarctic snowpack in central Alaska over a whole season. Consequences for the air to snow transfer of pollutants, *Environ. Sci. Technol.*, *40*, 7521–7527, doi:10.1021/es060842j.
- Villa, S., M. Vighi, V. Maggi, A. Finizio, and E. Bolzacchini (2003), Historical trends of organochlorine pesticides in an alpine glacier, *J. Atmos. Chem.*, *46*, 295–311.
- Wagner, C. (1961), Theorie der Alterung von Niederschlägen durch Umlösen, *Z. Elektrochem.*, *65*, 581–591.
- Warren, S. G. (1982), Optical properties of snow, *Rev. Geophys.*, *20*, 67–89.
- F. Domine and A.-S. Taillandier, Laboratoire de Glaciologie et Géophysique de l'Environnement, CNRS, BP 96, F-38402 Saint-Martin d'Hères Cedex, France. (florent@lgge.obs.ujf-grenoble.fr)
- T. A. Douglas and M. Sturm, U.S. Army Cold Regions Research and Engineering Laboratory, P.O. Box 35170, Fort Wainwright, AK 99703-0170, USA.
- W. R. Simpson, Geophysical Institute, University of Alaska Fairbanks, P.O. Box 757320, Fairbanks, AK 99775-7320, USA.